Insect. Soc. (2017) 64:209–217
DOI 10.1007/s00040-016-0533-8

Insectes Sociaux

RESEARCH ARTICLE

Structural and ultrastructural characterization of the spermatozoa in *Pachycondyla striata* and *P. marginata*

L. Cuquetto-Leite[1] · H. Dolder[1] · P. S. Oliveira[2] · N. B. Espírito Santo[2] · J. Lino-Neto[3] · K. C. Mancini[1,4]

Received: 24 March 2016 / Revised: 20 October 2016 / Accepted: 6 November 2016 / Published online: 2 December 2016
© International Union for the Study of Social Insects (IUSSI) 2016

Abstract This study characterizes the male gametic cells in two ant species (*Pachycondyla striata* and *Pachnoda marginata*) by light and transmission electron microscopies. The sperm of both species is composed of head, flagellum, and transition regions. The head consists of the acrosome, tapered and bilayer, and a cylindrical nucleus. In *P. marginata*, the intranuclear material is homogeneously compacted, and in *P. striata,* there are translucent inclusions and density variations. In the transition region of both species, centriolar adjunct, nuclear base, and the modified basal body (structure of the spermatozoa equivalent to the spermatids' centriole) coexist and are progressively replaced by two oval and symmetrical mitochondrial derivatives and an axoneme 9 + 9 + 2, respectively, in addition to two symmetrical triangular accessory bodies. Moreover, cytochemical analysis with Ethanolic Phosphotungstic Acid Method (E-PTA) revealed species-specific features not previously reported in the Formicidae, such as the presence of E-PTA negative acrosomal vesicle, E-PTA positive perforatorium, and E-PTA positive nucleus, all in *P. marginata*. Mitochondrial derivatives exhibited distinct behavior in its internal composition, with E-PTA negative mitochondrial cristae and E-PTA positive paracrystalline in both species. Sperm morphology in *Pachycondyla* has marked morphological similarities with other ant groups, and its specific features can be useful tools to understand phylogenetic relationships within the Formicidae and Hymenoptera.

Keywords Sperm cells · Ponerini · Ant · Morphology

✉ L. Cuquetto-Leite
livia.cuquetto@gmail.com

H. Dolder
dolder1207@gmail.com

P. S. Oliveira
pso@unicamp.br

N. B. Espírito Santo
nadiabes@gmail.com

J. Lino-Neto
linoneto@ufv.br

K. C. Mancini
karina.mancini@ufes.br

[1] Department of Structural and Functional Biology, Biology Institute, UNICAMP, Bertrand Russel Avenue, 13083-865 Campinas, São Paulo, Brazil

[2] Department of Animal Biology, Biology Institute, UNICAMP, Campinas, São Paulo, Brazil

[3] Department of General Biology, UFV, Viçosa, Minas Gerais, Brazil

[4] Department of Agricultural and Biological Sciences, UFES, São Mateus, Espírito Santo, Brazil

Introduction

As observed for many groups of insects (Phillips 1970; Dallai 1974, 2014; Jamieson 1987; Dallai and Afzelius 1993; Jamieson et al. 1999), sperm morphological characterization may be a relevant tool for understanding ant taxonomy and phylogenetic relationships within the Formicidae. In this context, some studies have focused on the morphology of the Hymenoptera spermatozoa, as it seems to be sufficiently varied among groups and conserved within species (Wheeler et al. 1990; Quicke et al. 1992; Newman and Quicke 1999a, b, 2000; Lino-Neto et al. 1999, 2000a, b; Lino-Neto and Dolder 2001a, b, 2002; Zama et al. 2001; Zama 2003). Although the family Formicidae has widely been studied in various aspects,

spermatic analysis is still required. The seven records reported in the literature represent only 15 of the 13.000 ant species described (Thompson and Blum 1967; Caetano 1980; Wheeler et al. 1990; Lino-Neto and Dolder 2002, 2008; Moya et al. 2007; Brunett and Heinze 2014).

Among Ponerinae tribes, the Ponerini shows weakly supported and controversial monophyletic features (Bolton et al. 2006; Moreau et al. 2006; Schmidt 2013), including the genus *Pachycondyla*. This genus includes a considerable amount of synonyms associated with few synapomorphies, which are responsible for its phylogenetic problems (Smith 2009; Mariano et al. 2011; Moreau and Bell 2013; Schmidt 2013; Schmidt and Shattuck 2014). Therefore, considering the importance of sperm characterization for understanding the systematics in insects, the reduced sperm data in Formicidae, as well as the existence of controversial phylogenetic characters in *Pachycondyla*, this study describes the spermatozoa of two *Pachycondyla* species.

Materials and methods

Males of *Pachycondyla marginata* and *Pachycondyla striata* were collected from excavated nests in the Santa Genebra Forest Reserve (Campinas, São Paulo, southeast Brazil), and in the campus of the Federal University of Viçosa (Viçosa, Minas Gerais, Brazil), respectively.

Drops of sperm suspension from the seminal vesicle were spread on histological slides and fixed with paraformaldehyde 4% in sodium phosphate buffer 0.1 M at room temperature. After fixation, the slides were quickly washed in tap water and dried. Then, they were examined and photographed in light microscope equipped with photographic camera. The measurements of the sperm average length were carried out with the Program Image Pro Plus, IPWin4.

For transmission electron microscopy analysis, testes and vesicles were dissected in sodium phosphate buffer and fixed in 2.5% glutaraldehyde and 4% paraformaldehyde for a period of 48 h at 4 °C. These fragments were washed in sodium phosphate buffer and postfixed in 1% osmium tetroxide for 2 h at room temperature. They were dehydrated in acetone series and embedded in epoxy resin at 60 °C for 72 h. Ultrathin sections were stained with aqueous solutions of 2% uranyl acetate and 0.1% lead citrate.

To improve the preservation of axonemal microtubules, testes and vesicles were fixed in 2.5% glutaraldehyde, 1% tannic acid, and 1.8% sucrose in 0.1 M sodium phosphate buffer for 3–5 days at 4 °C (Dallai and Afzelius 1990). This material was washed in the same buffer and stained with 2% aqueous uranyl acetate, in the dark, for 2 h at room temperature. Finally, the fragments were dehydrated, embedded, sectioned, and stained according to the protocol described above.

For detection of basic proteins, it was used the Ethanolic Phosphotungstic Acid method (E-PTA). Some materials were fixed in 2.5% glutaraldehyde solution in 0.1 M sodium phosphate buffer to which 1.5% sucrose was added. After washing in the respective buffer, they were dehydrated in increasing series of ethanol for 2 h at 4 °C and stained in 2% phosphotungstic acid with absolute ethanol for 2 h at room temperature (Modified from Bloom and Aghajanian 1968). Subsequently, the fragments were embedded and sectioned according with the protocol described above.

Results

Sperm morphology

The spermatozoa of *P. striata* and *P. marginata* are filiform, measuring about 130 and 200 μm in length, respectively (Figs. 1a, 2a). They are divided in two regions: the head measures about 20 μm in *P. striata* and 35 μm in *P. marginata*, and the flagellum measures about 105 and 160 μm in length, respectively (Figs. 1a, 2a). In both species, the head region consists of the acrosome in its anterior tip and the nucleus. The flagellum consists of an axoneme, two mitochondrial derivatives, and two accessory bodies. Both regions are interconnected by a transition portion.

The acrosome in both species is an elongated, tapered, and bilayer structure composed of an acrosomal vesicle—with 1.8 μm in length in *P. striata* and 1.0 μm in *P. marginata*, an internal perforatorium, and a slender translucent space between these two structures (Figs. 1b, 2b). The perforatorium measures about 1.5 μm in *P. striata* and 1.0 μm in *P. marginata*. In cross section of the acrosomal anterior tip of both species, it is observed an acrosomal vesicle followed by a perforatorium and translucent space, all of which present a circular shape (Figs. 1c, 2c, d). In the transverse section of the acrosomal posterior portion, the translucent space and the acrosomal vesicle acquire triangular shape, while the perforatorium maintains its circular shape. Although acrosomal shape alterations occur in both species, it is less prominent in *P. striata* compared to *P. marginata* (Figs. 1d, 2e). At its base, the acrosome presents an oblique contact with the nucleus, as the perforatorium extends to the nucleus anterior tip—for a length of 0.3 μm in *P. striata* and 0.2 μm in *P. marginata* (Figs. 1e, f, 2f, g). Cytochemical analyses showed that the acrosomal vesicle was E-PTA negative, whereas the perforatorium was E-PTA positive in *P. marginata* (Fig. 2h). In turn, in *P. striata*, the acrosome vesicle was E-PTA positive—although its initial portion has shown to be a pronounced E-PTA negative

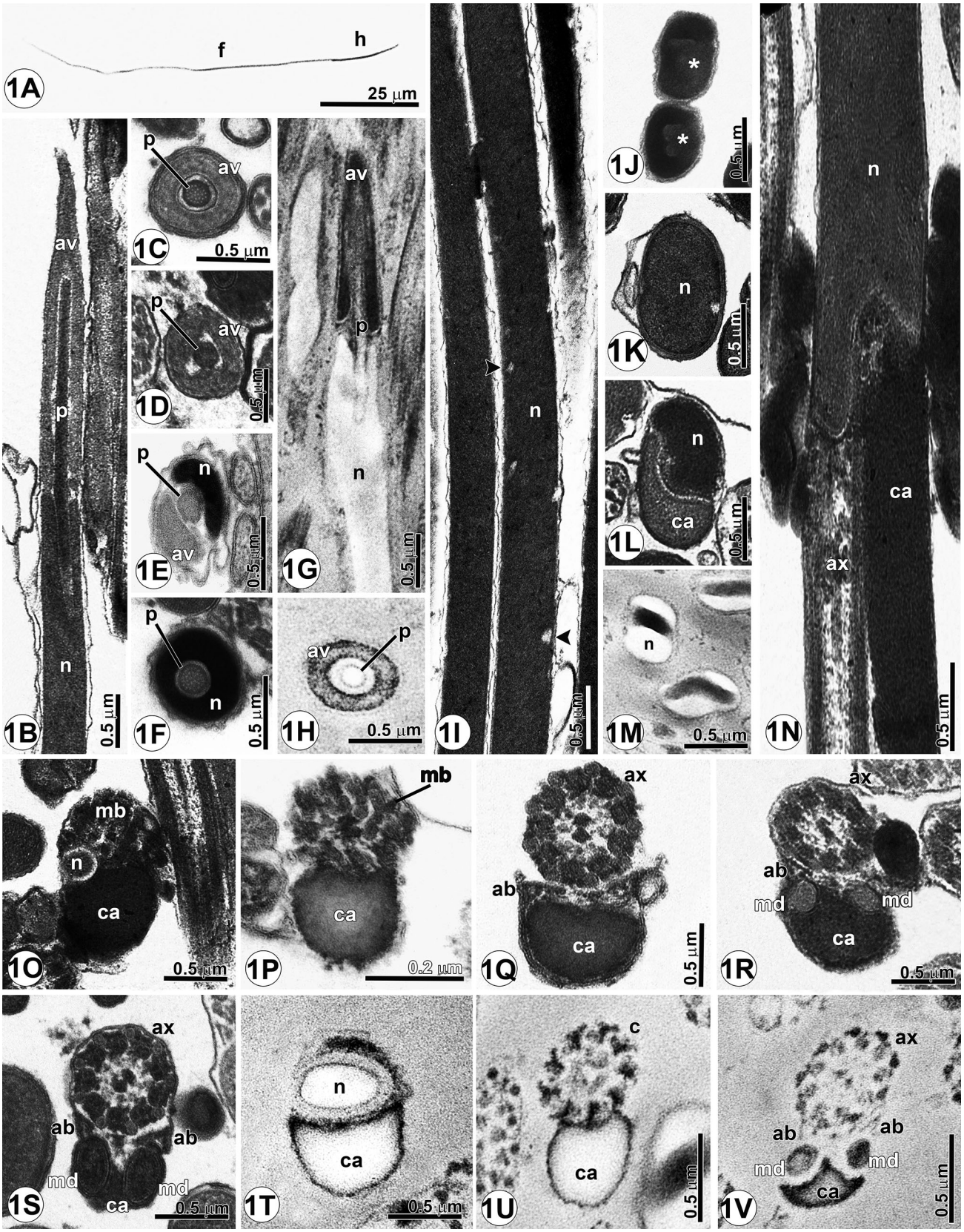
1A
f
h
25 μm
1B
av
p
n
0.5 μm
1C
p
av
0.5 μm
1D
p
av
0.5 μm
1E
p
n
av
0.5 μm
1F
p
n
0.5 μm
1G
av
p
n
0.5 μm
1H
av
p
0.5 μm
1I
n
0.5 μm
1J
*
*
0.5 μm
1K
n
0.5 μm
1L
n
ca
0.5 μm
1M
n
0.5 μm
1N
n
ca
ax
0.5 μm
1O
mb
n
ca
0.5 μm
1P
mb
ca
0.2 μm
1Q
ax
ab
ca
0.5 μm
1R
ax
ab
md
md
ca
0.5 μm
1S
ax
ab
ab
md
md
ca
0.5 μm
1T
n
ca
0.5 μm
1U
c
ca
0.5 μm
1V
ax
ab
ab
md
md
ca
0.5 μm

◀**Fig. 1** Spermatozoa of *P. striata*. **a** Light micrograph. **b** Longitudinal section of the anterior tip. **c–f** Serial cross sections of the acrosomal components. **g** E-PTA, longitudinal section of the anterior end. **h** E-PTA, acrosomal cross section. **i** Longitudinal section of the nucleus. **j–l** Serial nuclear cross sections, from the anterior to the posterior end. **m** E-PTA, cross section of the nucleus. **n** Longitudinal section of the transition nucleus–flagellum region. **o–s** Serial cross sections of the transition nucleus–flagellum region. **t–v** E-PTA, serial cross sections of the nucleus–flagellum transition region. *ab* accessory body, *av* acrosomal vesicle, *ax* axoneme, *mb* modified basal body, *ca* centriolar adjunct, *f* flagellum, *h* head, *md* mitochondrial derivative, *n* nucleus, *p* perforatorium, translucent inclusions (*arrowhead*) and density nuclear change (*)

structure (Fig. 1g, h)—and the perforatorium was E-PTA negative (Fig. 1g, h).

In both species, the nucleus is elongated and electron dense with high compacted chromatin (Figs. 1i, 2i). In *P. striata*, its anterior tip has a circular shape in cross section, which progressively acquires an oval shape (Fig. 1f, j, k), maintaining its diameter constant. In *P. marginata*, the nucleus remains circular in cross section for its entire extension, but the diameter increases toward the posterior end (Fig. 2i). In *P. striata*, the nucleus has areas with different densities, showing electron-lucid inclusions, which accumulate especially in the periphery (Fig. 1i–k). In cytochemical analyses, the nucleus of *P. striata* was E-PTA negative, with high positivity in some areas (Fig. 1g, m). On the other hand, in *P. marginata*, the nucleus was slight E-PTA positive in its entire extension (Fig. 2j, k).

In the transition region, the nuclear posterior portion is oblique with a protrusion of 1.6 µm in length in *P. striata* (Fig. 1l, n), and 2.2 µm in *P. marginata* (Fig. 2l). In both species, this nuclear portion is of semicircular shape and rests on the anterior concave base of the centriolar adjunct (Figs. 1l, 2m). The nuclear posterior tip progressively reduces in diameter, showing a small circle partly surrounded by the anterior tip of the modified basal body—both juxtaposed to the concavity of the centriolar adjunct. In its anterior portion, the centriolar adjunct has a semicircular shape in *P. striata* and an ovoid shape in *P. marginata* (Figs. 1o, p, 2n, o). In both species, the axoneme is formed from the modified basal body with a 9 + 9 + 0 microtubular configuration that turns into a 9 + 9 + 1 and, finally, a 9 + 9 + 2 configuration, as it approaches the flagellum (Fig. 2o–r). In this region, it is possible to observe the beginning of accessory bodies and mitochondrial derivatives between axoneme and centriolar adjunct (Fig. 2q, r). The mitochondrial derivatives, in its initial portions, are symmetrical to each other and increase in diameter as they occupy the centriolar adjunct space (Figs. 1r, s, 2r). By the E-PTA technique, the structures of the transition region showed different behaviors between the studied species. In *P. striata*, the centriolar adjunct was E-PTA negative, except in its periphery, becoming E-PTA positive in its posterior portion, especially with the emergence of mitochondrial derivatives (Fig. 1t–v). In turn, in *P. marginata*, the centriolar adjunct was intense E-PTA negative in its luminal region and E-PTA positive in its periphery along its entire length (Fig. 2s, t). In both species, accessory bodies were E-PTA negative and the anterior tip of the mitochondrial derivatives was positive (Figs. 1v, 2u).

The flagellum of both species is characterized by axoneme with 9 + 9 + 2 microtubular arrangement (with 16 protofilaments in the accessory microtubule) (*inset,* Fig. 3a, h), two symmetrical mitochondrial derivatives (oval in *P. striata* and pyriform in *P. marginata*, in cross section), and two symmetrical and triangular accessory bodies, in transverse section (Fig. 3a, f). Along the flagellum, except in its posterior portion, the mitochondrial derivatives in both species differ in the configuration of their two internal contents. In *P. marginata,* they exhibit a granular area of low density, corresponding to the paracrystalline material proximal to the axoneme, and a greater density area corresponding to the mitochondrial cristae (Fig. 3a). In turn, in *P. striata*, the mitochondrial derivatives exhibit a dense paracrystalline area proximal to the axoneme, whereas the mitochondrial cristae are electron lucid (Fig. 3f). Along the flagellum, both accessory bodies present triangular shape, in transverse section, with the periphery poor electron dense and filled with low density amorphous material (Fig. 3a, f). In cytochemical analyses, in both species, the microtubules of the axoneme are E-PTA positive, especially the accessory tubules. In the central pair, both luminal and radius justaxonemal portions are positive (Fig. 3b, l). The mitochondrial derivatives exhibit specific E-PTA reaction for each species. In *P. marginata,* only the mitochondrial cristae region is E-PTA negative (Fig. 3b). In contrast, in *P. striata*, the mitochondrial proximal area to the axoneme seemed to be strongly E-PTA positive, different from the distal one. In this distal region, its outline was E-PTA positive, as well as the mitochondrial derivative membrane. The mitochondrial middle portion was E-PTA negative (Fig. 3l).

At the distal end of the flagellum, the configuration of components differs between the species. In *P. striata*, one mitochondrial derivative ends before the other (Fig. 3g–k). The microtubules of the central pair are the first to end, before the mitochondrial derivatives and accessory bodies, resulting in a 9 + 9 + 0 microtubule arrangement. The mitochondrial derivatives disappear in different levels, followed by accessory bodies, and finally, the axoneme remains with only the accessory microtubules (Fig. 3g–k). On the other hand, in *P. marginata*, the mitochondrial derivatives and accessory bodies end together and before any axonemal disarrangement (Fig. 3c–e).

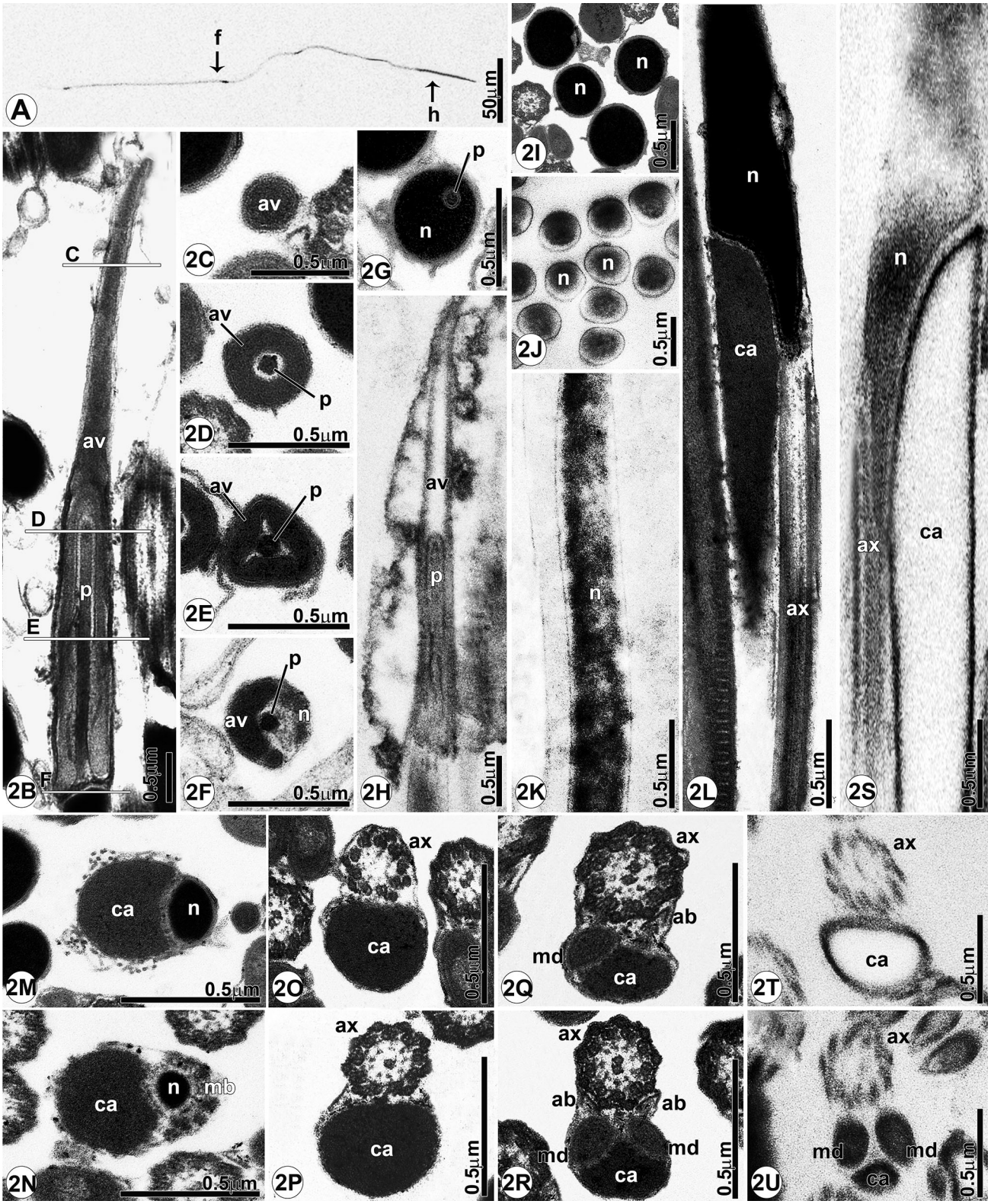
A
f
h
50µm
2B
C
D
E
F
av
p
0.5µm
2C
av
0.5µm
2D
av
p
0.5µm
2E
av
p
0.5µm
2F
p
av
n
0.5µm
2G
p
n
0.5µm
2H
av
p
0.5µm
2I
n
n
0.5µm
2J
n
n
0.5µm
2K
n
0.5µm
2L
n
ca
ax
0.5µm
2S
n
ax
ca
0.5µm
2M
ca
n
0.5µm
2O
ax
ca
0.5µm
2Q
ax
ab
md
ca
0.5µm
2T
ax
ca
0.5µm
2N
ca
n
mb
0.5µm
2P
ax
ca
0.5µm
2R
ax
ab
ab
md
md
ca
0.5µm
2U
ax
md
md
ca
0.5µm

◀**Fig. 2** Spermatozoa of *P. marginata*. **a** Light micrograph. **b** Longitudinal acrosomal section. **c–g** Serial cross section of the acrosomal components. **h** E-PTA, longitudinal section of the acrosome. **i** Cross section of nuclear portion. **j** E-PTA, cross section of the nuclear portion. **k** E-PTA, longitudinal section of the nucleus. **l** Longitudinal section of the nucleus–flagellum transition region. **m–r** Serial cross sections of the nucleus–flagellum transition portion. **s** E-PTA, longitudinal section of the nucleus–flagellum transition region. **t–u** E-PTA, cross sections of the nucleus–flagellum transition. *ab* accessory bodies, *av* acrosomal vesicle, *ax* axoneme, *mb* modified basal body, *ca* centriolar adjunct, *f* flagellum, *h* head, *md* mitochondrial derivatives, *n* nucleus, *p* perforatorium

Discussion

Both *Pachycondyla* species analyzed differ from each other in relation to the chromatin configuration. The nucleus in *P. marginata* displays a homogeneously compact chromatin, whereas scattered electron-lucid inclusions are observed in *P. striata*. Similar inclusions were also reported for *Solenopsis invicta* (Lino-Neto and Dolder 2002) and *Pseudomyrmex penetrator* (Moya et al. 2007). In *P. penetrator*, in addition to the inclusions, intense unpacking chromatin occurs at the nuclear periphery. The chromatin configuration with electron-lucid inclusions observed in *P. striata* exhibited a specific pattern to the species, never observed to other Hymenoptera, which suggests that could be an autapomorphy of the species.

The penetration of the nuclear distal portion in the centriolar initial base is not reported for most Apoidea, including Formicidae (Caetano 1980; Lino-Neto and Dolder 2002; Zama et al. 2001, 2004, 2005a, b; Báo et al. 2004; Fiorillo et al. 2005a, b; Moya et al. 2007; Lino-Neto et al. 2008). In addition, in *Pachycondyla*, this region exhibits configuration different from Apidae (Peng et al. 1993; Lino-Neto et al. 2000b; Gracielle et al. 2009; Gomes et al. 2012) and Vespidae (Mancini et al. 2006, 2009; Moreira et al. 2012), since in Apidae, the nucleus is surrounded by the modified basal body, while in Vespidae, the beginning of longer mitochondrial derivative acts as base. Therefore, these character states could be synapomorphies of the genus *Pachycondyla*, considering the specific provision of this region in each *Pachycondyla*.

The presence of a symmetrical centriolar adjunct, situated between the nucleus base and the anterior end of both mitochondrial derivatives, as noted in these *Pachycondyla* species, is common to Formicidae (Caetano 1980; Wheeler et al. 1990; Lino-Neto and Dolder 2002; Moya et al. 2007; Lino-Neto et al. 2008). Although this character state is shared with Symphyta Siricoidea (Newman and Quicke 1999a) and Parasitica Chalcidoidea (Lino-Neto et al. 1999, 2000b; Lino-Neto and Dolder 2001b), in most Aculeata, this structure is located between the nucleus and only one mitochondrial derivative (Zama et al. 2004, 2005b, 2007; Araujo et al. 2005; Fiorillo et al. 2005b; Gracielle et al. 2009; Mancini et al. 2006, 2009). Therefore, considering that Formicidae is recognized as a family derived from Aculeata, it is possible to suppose that the symmetric condition of the adjunct may have been expressed more than once in Hymenoptera.

Although the spermatozoa of *Pachycondyla* present flagellar configuration commonly observed in Hymenoptera, they also show some variation. In both species, mitochondrial derivatives exhibit traits that differ from other Aculeata and relate them to Formicidae. The mitochondrial derivatives of ants show shapes ranging from ovoid to pear shape, similar diameter in cross sections and presence of paracrystalline material proximal to the axoneme (Caetano 1980; Wheeler et al. 1990; Lino-Neto and Dolder 2002; Moya et al. 2007; Lino-Neto et al. 2008). However, several groups phylogenetically distant from Formicidae—such as Eucoilidae, Megalyroidea (Newman and Quicke 1999b, 2000; Gracielle et al. 2009; Gomes et al. 2012), Apidae (Lino-Neto et al. 2000b; Zama et al. 2001, 2004, 2005a; Báo et al. 2004), and Halictidae (Fiorillo et al. 2005a, b)—and Vespidae (Mancini et al. 2006, 2009; Moreira et al. 2012)—which is a group phylogenetically similar to Formicidae—exhibit asymmetry in their mitochondrial derivatives.

In the terminal region, the end of the mitochondrial derivatives with the perfectly organized axoneme, as observed in *P. marginata*, has been observed in other Formicidae, but the end of the derivatives after the disarrangement of the central pair, as observed in *P. striata*, was reported only in *Pseudomyrmex* (Moya et al. 2007). In *P. marginata*, the microtubule disorganization in the final flagellum region is preceded by a change in the disposition of the intertubular material that can be specific to the species, since it was not reported to other Formicidae species, or even to other Hymenoptera.

This study is the first to perform cytochemical analyses of spermatozoa in the Formicidae, finding relevant differences between the species studied and with respect to some Hymenoptera. Whereas in *P. striata*, E-PTA was positive only in the central region—as described for Meliponini Apidae and Euglossini Bombini (Zama 2003; Zama et al. 2001, 2004, 2005a), in *P. marginata,* basic proteins were observed across the entire nuclear area, a feature not yet reported for any other Hymenoptera. The variation of E-PTA negative in the anterior portion and positive at the distal end exhibited by centriolar adjunct in *P. striata* was never reported to any Hymenoptera, and could be an autapomorphy in this species. The mitochondrial derivatives presented different reaction to E-PTA not yet

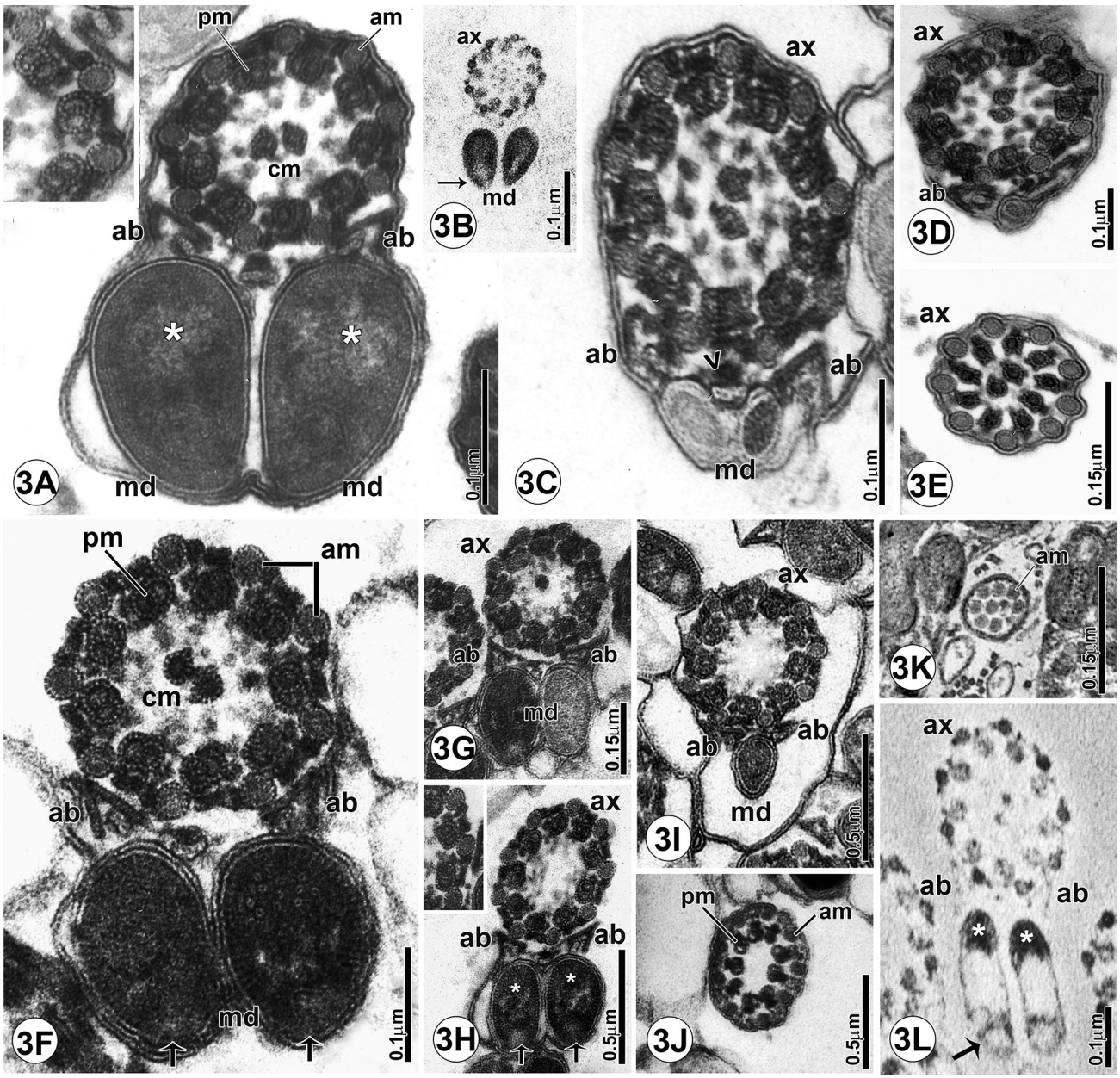

Fig. 3 Spermatozoa of *P. marginata* and *P. striata* (Transmission electron microscopy). *Pachnoda marginata*—**a** cross section of the flagellar portion. Note the protofilaments in detail. **b** E-PTA, cross section of the flagellar components. **c–e** Serial cross sections of the flagellar end. *Pachycondyla striata*—**f** flagellar cross section. **g–k** Serial cross sections of the flagellar end; **h** note the protofilaments in detail. **l** E-PTA, flagellar cross section. *ab* accessory bodies, *am* microtubules accessories, *ax* axoneme, *cm* central microtubules, *md* mitochondrial derivatives, *pm* peripheral microtubules, paracrystalline (*), mitochondrial cristae (*arrow*), material between derivatives (*arrowhead*)

described for Hymenoptera, including Formicidae, having the same potential to act as a species-specific character.

The characters shown by both species, *P. marginata* and *P. striata*, are widely consistent with the data displayed by the Formicidae already studied, when considered: (1) acrosomal components, (2) centriolar adjunct disposal in relation to mitochondrial derivatives and (3) shape, cross symmetry, and distribution of the internal content of mitochondrial derivatives. The sharing of these characters highlights the existence of a morphological pattern for Formicidae. In addition, other traits suggest the presence of additional synapomorphies between *Pachycondyla* species, such as the arrangement of components in the transition region, giving further support for the monophyly of the genus. Other characters have the potential to be used in future studies of *Pachycondyla* systematics, such as the

distribution pattern of the internal content of mitochondrial derivatives and density variations of the chromatin material (especially observed in *P. striata*). The characters described represent a potential tool for the phylogeny of *Pachycondyla* and Formicidae, although more representative analyses of the genus and family are necessary to define phylogenetic relationships more precisely.

Acknowledgements The authors thank the Laboratories of Reproductive Biology and Electron Microscopy of the Biology Institute/Unicamp. Paulo S. Oliveira was supported by grants from FAPESP (11/18580-8, 12/23671-5, 14/23141-1) and CNPq (306115/2013-1). Nádia Espírito Santo was supported by fellowships from CNPq and CAPES. We thank André Freitas for helpful suggestions on the final version of the manuscript.

References

Afzelius BA, Dallai R (1990) Microtubular diversity in insect spermatozoa: results obtained with a new fixative. J Struct Biol 103:164–179

Araujo VA, Zama U, Dolder H, Lino-Neto J (2005) Morphology and ultrastructure of the spermatozoa of *Scaptotrigona xanthotricha* Moure (Hymenoptera Apidae Meliponini). Braz J Morphol Sci 22:137–141

Báo SN, Gonçalves Simões D, Lino-Neto J (2004) Sperm ultrastructure of the bees *Exomalopsis* (Exomalopsis) *auropilosa* Spinola 1853 and *Paratetrapedia* (Lophopedia) sp. Michener and Moure 1957 (Hymenoptera Apidae, Apinae). J Submicrosc Cytol Pathol 36:23–28

Bloom FE, Aghajanian GK (1968) Fine structural and cytochemical analysis of the staining of synaptic junctions with phosphotungstic acid. J Ultrastruct Res 22:361–375

Bolton B, Alpert G, Ward PS, Naskrecki P (2006) Bolton's catalogue of ants of the world: 1758–2005.CD-ROM. Harvard University Press, Cambridge

Brunett WE, Heinze J (2014) Sperm bundles in the seminal vesicles of sexually mature *Lasius* ant males. PLoS One 9(3):e93383

Caetano FH (1980) Ultra-estrutura dos espermatozoides de *Atta capiguara e Atta sexdens rubropilosa* (Formicidae). Naturalia 5:105–111

Dallai R (1974) Spermatozoa and phylogenesis. A few data on insecta apterygota. Pedobiology 14:148–156

Dallai R (2014) Overview on spermatogenesis and sperm structure of Hexapoda. Arthropod Struct Dev 43:257–290

Dallai R, Afzelius BA (1993) Development of the accessory tubules of insect sperm flagella. J Submicrosc Cytol Pathol 25:499–504

Fiorillo BS, Lino-Neto J, Báo SN (2005a) Ultrastructural characterization of the spermatozoon of *Xylocopa frontalis* (Hymenoptera, Anthophoridae). Braz J Morphol Sci 22:60–61

Fiorillo BS, Coelho AM, Lino-Neto J, Báo SN (2005b) Structure and ultrastructure of the spermatozoa of Halictidae (Hymenoptera, Apoidea). J Submicrosc Cytol Pathol 37:75–81

Gomes LF, Badke JP, Zama U, Dolder H, Lino-Neto J (2012) Morphology of the male reproductive system and spermatozoa in *Centris* Fabricius, 1804 (Hymenoptera: Apidae, Centridini). Micron 43:695–704

Gracielle IMS, Fiorillo BS, Lino-Neto J, Báo SN (2009) Morphology of the male reproductive system and spermiogenesis in *Hypanthidium foveolatum* (Alfken, 1930) (Hymenoptera: Apidae, Megachilinae). Micron 40:719–723

Jamieson BGM (1987) The ultrastructure and phylogeny of insect spermatozoa. Cambridge University Press, Cambridge, pp 320–329

Jamieson BGM, Dallai R, Afzelius BA (1999) Insects: their spermatozoa and phylogeny. Science Publishers, Enfield, p 555

Lino-Neto J, Dolder H (2001a) Redescription of sperm structure and ultrastructure of *Trichogramma dendrolini* (Hymenoptera: Chalcidoidea: Trichogrammatidae). Acta Zool 82:159–164

Lino-Neto J, Dolder H (2001b) Structural characteristics of the spermatozoa of Scelionidae (Hymenoptera; Platygastroidea) with phylogenetic considerations. Zool Scr 30:89–96

Lino-Neto J, Dolder H (2002) Sperm structure and ultrastructure of the fire ant *Solenopsis invicta* (Buren) (Hymenoptera, Formicidade). Tissue Cell 34:124–128

Lino-Neto J, Báo SN, Dolder H (1999) Structure and ultrastructure of spermatozoa of *Bephratelloides pomorum* (Fabricius) (Hymenoptera: Euritomidae). Int J Insect Morphol 28:253–259

Lino-Neto J, Báo SN, Dolder H (2000a) Structure and ultrastructure of spermatozoa of *Trichogramma pretiosum* Riley and *Trichogramma atopovirilia* Oatma and Platner (Hymenoptera: Trichogrammatidae). Acta Zool 81:205–211

Lino-Neto J, Báo SN, Dolder H (2000b) Sperm ultrastructure of the honey bee (*Apis mellifera*) (L) (Hymenoptera, Apidae) with emphasis on the nucleus-flagellum transition region. Tissue Cell 32:322–327

Lino-Neto J, Zama U, Mancini K (2008) Morfologia dos Espermatozoides de Hymenoptera. In: Vilela EF, Santos IA, Schoereder JH, Serrão JE, Campos LAO, Lino-Neto J (eds) Insetos sociais: da biologia a aplicação. UFV, Viçosa, pp 150–173

Mancini K, Lino-Neto J, Campos LAO, Dolder H (2006) Sperm ultrastructure of *Agelaia vicina* (Hymenoptera Vespidae). Insect Soc 53:333–338

Mancini K, Lino-Neto J, Dolder H, Dallai R (2009) Sperm ultrastructure of the European hornet *Vespa crabro* (Linnaeus, 1758) (Hymenoptera Vespidae). Arthropod Struct Dev 38:54–59

Mariano CSF, Pompolo SDG, Silva JG, Delabie JHC (2011) Contribution of cytogenetics to the debate on the paraphyly of *Pachycondyla* spp. (Hymenoptera, Formicidae, Ponerinae). Psyche 2012:1–9

Moreau CS, Bell CD (2013) Testing the museum versus cradle tropical biological diversity hypothesis: phylogeny, diversification, and ancestral biogeographic range evolution of the ants. Evol 67:2240–2257

Moreau CS, Bell CD, Vila R, Archibald SB, Pierce NE (2006) Phylogeny of the ants: diversifiation in the age of angiosperms. Science 312:101–104

Moreira J, Brito P, Mancini K, Dolder H, Lino-Neto J (2012) The descriptions of new microanatomical structure of the male reproductive system and sperm of *Myschocyttarus cassununga* (Hymenoptera: Vespidae). Micron 43:292–297

Moya J, Mancini K, Lino-Neto J, Delabie J, Dolder H (2007) Sperm ultrastructure of five species of the Neotropical ant genus *Pseudomyrmex* (Hymenoptera Formicidae). Acta Zool 88:181–187

Newman TM, Quicke DLJ (1999a) Ultrastructure of imaginal spermatozoa of sawflies (Hymenoptera: Symphyta). J Hymenopt Res 8:35–47

Newman TM, Quicke DLJ (1999b) Ultrastructure of spermatozoa in *Leptopilina* (Hymenoptera: Cynipoidea: Eucoilidae). J Hymenopt Res 8:197–203

Newman TM, Quicke DLJ (2000) Sperm development and ultrastructure of mature spermatozoa of Megalyra (Hymenoptera: Megalyroidea). J Hymenopt Res 9:62–70

Peng CYS, Yin CM, Yin LRS (1993) Ultrastructure of honey bee *Apis mellifera*, sperm with special emphasis on the acrosomal complex

following high-pressure freezing fixation. Physiol Entomol 18:93–101

Phillips DM (1970) Insect sperm: their structure and morphogenesis. J Cell Biol 44:243–277

Quicke DLJ, Ingram SN, Baillie HS, Gaitens PV (1992) Sperm structure and ultrastructure in the Hymenoptera (Insecta). Zool Sci 21:381–402

Schmidt C (2013) Molecular phylogenetics of ponerine ants (Hymenoptera: Formicidae: Ponerinae). Zootaxa 3647:201–250

Schmidt CA, Shattuck SO (2014) The higher classification of the ant subfamily Ponerinae (Hymenoptera: Formicidae), with a review of ponerine ecology and behavior. Zootaxa 3817:1–242

Smith CA (2009) Molecular phylogenetics and taxonomic revision of ponerine ants. PhD dissertation, University of Arizona, Tucson, Az, p 279

Thompson TE, Blum MS (1967) Structure and behavior of spermatozoa of fire ant *Solenopsis saevissima* (Hymenoptera–Formicidae). Ann Entomol Soc Am 60:632–642

Wheeler DE, Crichton EG, Krutzsch PH (1990) Comparative ultrastructure of ant spermatozoa (Formicidae: Hymenoptera). J Morphol 206:343–350

Zama U (2003) Estudo estrutural e ultraestrutural dos espermatozóides nas Tribos Apini, Bombini, Euglossini e Meliponini (Hymenoptera: Apinae), com considerações filogenéticas. PhD thesis, State University of Campinas

Zama U, Lino-Neto J, Dolder H (2001) Ultrastructure of spermatozoa in *Plebeia* (Plebeia) *droryana* Friese (Hymenoptera: Apidae, Meliponina). J Hymenopt Res 10:261–270

Zama U, Lino-Neto J, Dolder H (2004) Structure and ultrastructure of spermatozoa in Meliponini (stingless bees) (Hymenoptera: Apidae). Tissue Cell 36:29–41

Zama U, Brito P, Lino-Neto J, Campos LAO, Dolder H, Báo SN (2005a) The sperm morphology of mud dauber *Sceliphron fistularium* Dahlbom (Hymenoptera: Apoidea: Sphecidae), as an indicative of bees relation. J Submicrosc Cytol Pathol 37:313–321

Zama U, Lino-Neto J, Melo SM, Campos LAO, Dolder H (2005b) Ultrastructural characterization of spermatozoa in Euglossine bees (Hymenoptera: Apidae, Apinae). Insect Soc 52:122–131

Zama U, Moreira J, Báo SN, Campos LAO, Dolder H, Lino-Neto J (2007) Morphology of testicular and post-testicular spermatozoa in *Microstigmus arlei* Richards 1972 and *M. nigrophthalmus* Melo, 1992 (Hymenoptera, Apoidea, Pemphredoninae) with phylogenetic consideration. Arthropod Struct Dev 36:304–316